

## Supplementary Material

### Field Induced Single Ion Magnetic Behaviour in Square-pyramidal Cobalt(II) Complexes with Easy-plane Magnetic Anisotropy

**Table S1.** X-ray Crystallographic Data and Refinement Parameters for complexes **1** and **2**.

	<b>1</b>	<b>2</b>
Formula	C <sub>14</sub> H <sub>32</sub> ClCoN <sub>4</sub> F <sub>4</sub> B	C <sub>38</sub> H <sub>47</sub> Cl <sub>2</sub> CoN <sub>5</sub> O <sub>4</sub>
M <sub>w</sub> (g mol <sup>-1</sup> )	437.63	767.64
Crystal size (mm)	0.50×0.19×0.15	0.44×0.16×0.15
Crystal system	Monoclinic	Monoclinic
Space group	<i>P</i> 2 <sub>1</sub>	<i>C</i> 2/ <i>c</i>
T (K)	148(2)	139(2)
a (Å)	8.2356(12)	34.573(3)
b (Å)	14.849(2)	14.1926(11)
c (Å)	8.4147(14)	16.0044(11)
(°)	90.00	90.00
(°)	109.245(8)	113.669(4)
(°)	90.00	90.00
V (Å <sup>3</sup> )	971.5(3)	7192.5(10)
Z	2	8
ρ <sub>calcd</sub> (g cm <sup>-3</sup> )	1.496	1.417
μ(MoKα) (mm <sup>-1</sup> )	1.062	0.674
F(000)	458.0	3224.0
T <sub>max</sub> , T <sub>min</sub>	0.863, 0.775	0.914, 0.889
h, k, l range	-10 ≤ h ≤ 10, -18 ≤ k ≤ 18, -10 ≤ l ≤ 10	-46 ≤ h ≤ 46, -19 ≤ k ≤ 19, -21 ≤ l ≤ 21
Collected reflections	2908	6696
Independent reflections	2316	6082
Goodness-of-fit (GOF) on F <sup>2</sup>	1.064	1.011
R1, wR2 (I > 2σI)	0.0636, 0.1576	0.0617, 0.1613
R1, wR2 (all data)	0.0849, 0.1673	0.0672, 0.1667
CCDC Number	1458031	1455062

$$R1 = \frac{\sum ||F_o| - |F_c||}{\sum |F_o|} \text{ and } wR2 = \frac{|\sum w(|F_o|^2 - |F_c|^2)|}{\sum w(F_o)^2}^{1/2}$$

**Table S2.** Bond distances (Å) and bond angles (°) around Co<sup>II</sup> centers found in complex **1** and **2**.

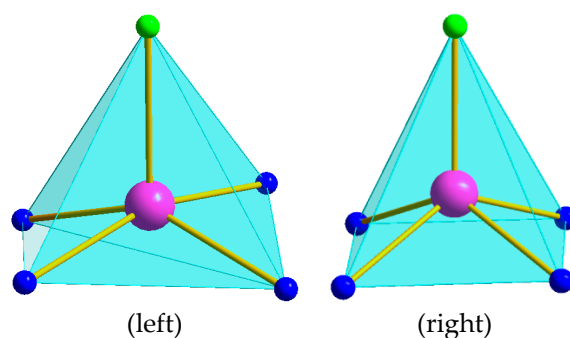
Bond distance (Å)					
<b>Complex 1</b>	Co – N1	2.1518(1)	<b>Complex 2</b>	Co – N2	2.1485(1)
	Co – N2	2.1972(1)		Co – N3	2.1808(1)
	Co – N3	2.1433(1)		Co – N4	2.1541(1)
	Co – N4	2.1618(1)		Co – N5	2.1754(1)
	Co – Cl1	2.2850(1)		Co – Cl2	2.2447(1)
Bond angle (°)					
<b>Complex 1</b>	Cl1–Co1–N2	98.91(6)	<b>Complex 2</b>	Cl2–Co1–N2	115.38(4)
	Cl1–Co1–N1	105.48(5)		Cl2–Co1–N3	105.45(4)
	Cl1–Co1–N4	98.33(5)		Cl2–Co1–N5	118.47(4)
	Cl1–Co1–N3	108.07(5)		Cl2–Co1–N4	108.62(6)
	N2–Co1–N1	91.26(6)		N2–Co1–N3	81.59(6)
	N2–Co1–N4	162.74(6)		N2–Co1–N5	82.28(5)
	N2–Co1–N3	82.71(5)		N2–Co1–N4	135.62(4)
	N1–Co1–N4	83.36(5)		N3–Co1–N5	135.99(5)
	N1–Co1–N3	146.43(5)		N3–Co1–N4	81.63(4)
	N4–Co1–N3	92.72(6)		N5–Co1–N4	81.96(4)

Shape analysis

**Table S3.** Summary of SHAPE analysis for complexes **1-2**.

PP-5	1	D <sub>5h</sub>	Pentagon
vOC-5	2	C <sub>4v</sub>	Vacant octahedron
TBPY-5	3	D <sub>3h</sub>	Trigonal bipyramid
SPY-5	4	C <sub>4v</sub>	Spherical square pyramid
JTBPY-5	5	D <sub>3h</sub>	Johnson trigonal bipyramid J12

Structure [ML <sub>5</sub> ]	PP-5	vOC-5	TBPY-5	SPY-5	JTBPY-5
Complex <b>1</b>	32.439	2.186	3.037	<b>0.558</b>	5.891
Complex <b>2</b>	32.028	4.674	5.931	<b>0.846</b>	9.781

**Figure S1.** Distorted square-pyramidal coordination geometry around the Co<sup>II</sup> centers in **1** (left) and **2** (right).

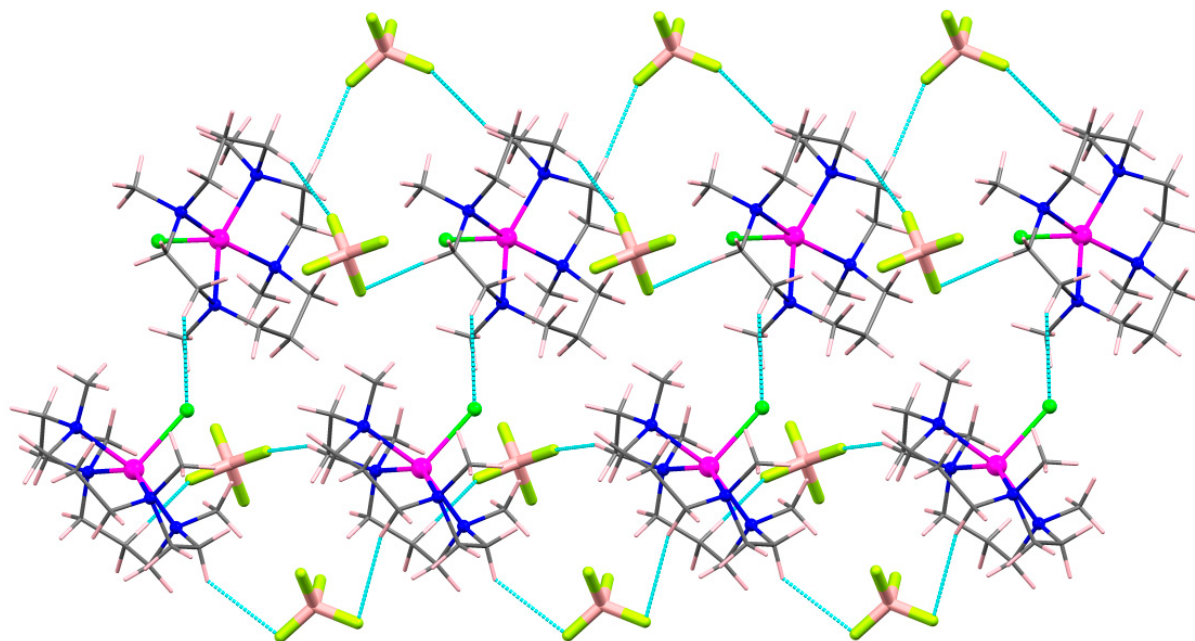


**Figure S2.** A view of supramolecular 2D arrangement of complex **1** through intermolecular H-bonding interactions.

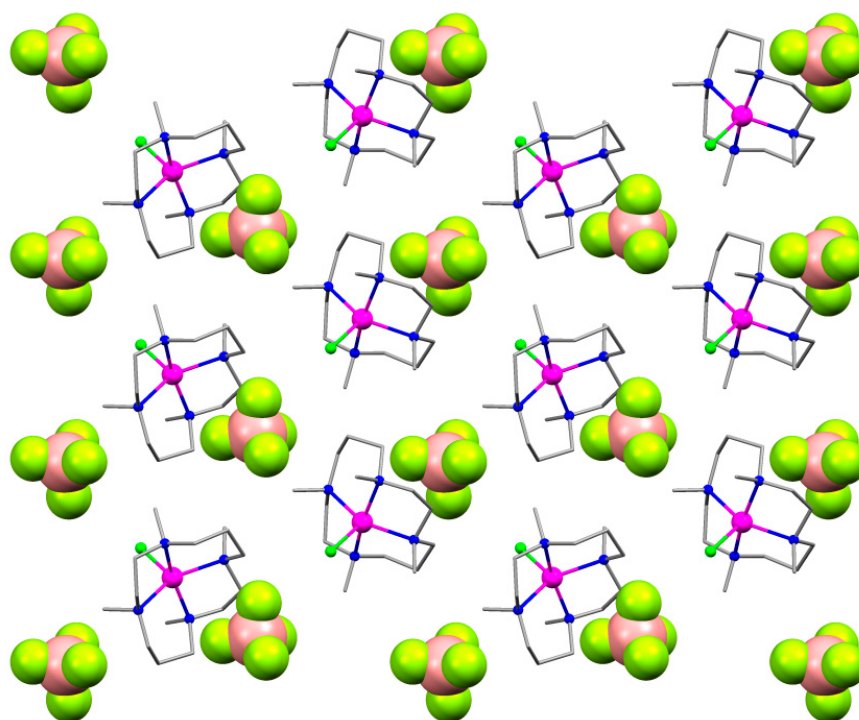


**Figure S3.** A view of packing diagram of complex **1** illustrating the continuous 2D arrangement of counter anions along the crystallographic *a*-axis.

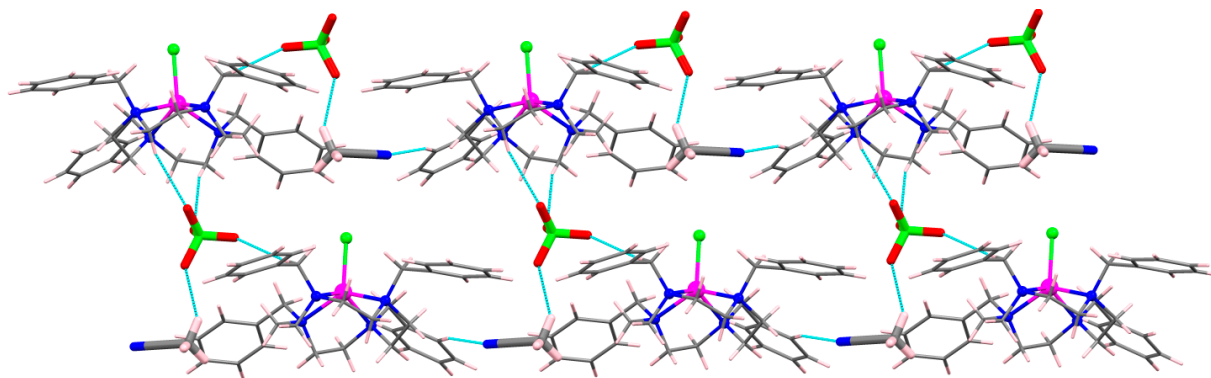


**Figure S4.** A view of supramolecular 2D arrangement of complex 2 through intermolecular H-bonding interactions.

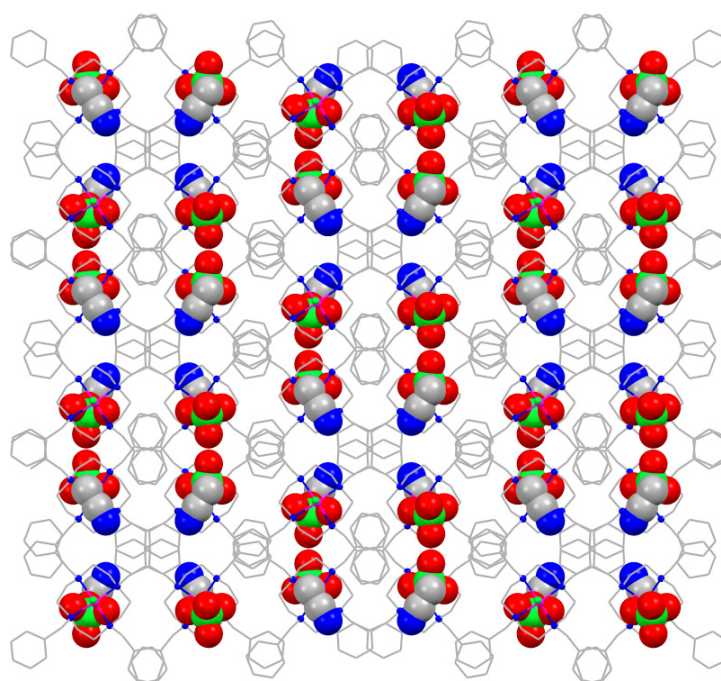


**Figure S5.** A view of packing diagram of complex 2 illustrating the continuous 2D arrangement of lattice solvent molecules and counter anions along the crystallographic *c*-axis.

**Table S4.** H-bond parameters found in complex 1.

D–H...A	D–H(Å)	H...A(Å)	D...A (Å)	<D–H–A(°)	Symmetry <sup>#</sup>
C6–H6A...C11	0.980	2.580	3.239	125.00	0
C1–H1B...F4	0.990	2.520	3.348	141.00	1
C9–H9B...F1	0.990	2.410	3.365	162.00	1
C8–H8B...C11	0.990	2.790	3.728	159.00	2
C10–H10A...F3	0.990	2.430	3.382	161.00	3
C14–H14B...F4	0.990	2.520	3.130	120.00	4

<sup>#</sup> (0) *x,y,z*; (1) 1-*x*,1/2+*y*,1-*z*; (2) *x,y*,1+*z*; (3) -1+*x,y*,1+*z*; (4) 2-*x*,1/2+*y*,1-*z*.

**Table S5.** H-bond parameters found in complex 2.

D–H...A	D–H(Å)	H...A(Å)	D...A(Å)	<D–H–A(°)	Symmetry <sup>#</sup>
C31–H31B...O1	0.990	2.440	3.305	146.00	0
C22–H22A...O4	0.990	2.570	3.530	163.00	1
C37–H37C...O3	0.980	2.500	3.316	140.00	1

<sup>#</sup> (0) x,y,z; (1) x,1-y,1/2+z.

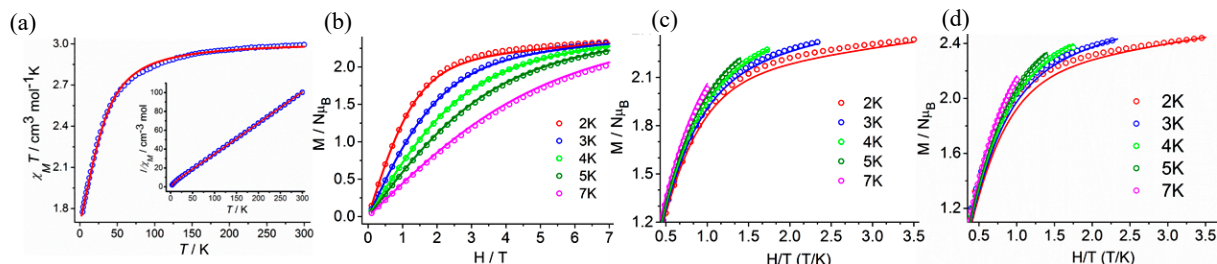


**Figure S6.**  $\chi_M T$  vs.  $T$  plots measured at 0.1 T for complex 1 (a).  $1/\chi_M$  vs.  $T$  plots shown in the inset;  $M/N\mu_B$  vs.  $H$  plots for complex 1 (b) at the indicated temperatures. The solid lines are the best fit;  $M/N\mu_B$  vs.  $H/T$  plots at the indicated temperatures for complexes 1 (c) and 2 (d). The solid lines are the best fit.

**Table S6.** Magnetic anisotropy ( $D$  parameter) and SIM parameters for previously reported pentacoordinate  $\text{Co}^{\text{II}}$  single ion magnets (SIMs).

Complex	Coordination geometry around $\text{Co}^{\text{II}}$ center	$D$ ( $\text{cm}^{-1}$ )	$U^{\text{eff}}$ ( $\text{cm}^{-1}$ )	$\tau_0$ (s)	Ref.
$[\text{Co}^{\text{II}}(\text{tbta})\text{N}_3](\text{ClO}_4)$	Trigonal bipyramidal	-10.7	19.7	$1.6 \times 10^{-8}$	1
$[\text{Co}^{\text{II}}(\text{bzimpy})\text{Cl}_2]$	Trigonal bipyramidal	71.7	nr	nr	2
$[\text{Co}^{\text{II}}(\text{Idppy})\text{Cl}_2]$	Trigonal bipyramidal	71.7	nr	nr	3
$[\text{Co}^{\text{II}}(\text{ddppy})\text{Cl}_2]$	Trigonal bipyramidal	71.7	nr	nr	3
$[\text{Co}(\text{phen})(\text{DMSO})\text{Cl}_2]$	Trigonal bipyramidal	-17.0	10.4	$5.6 \times 10^{-9}$	4
$[\text{Co}^{\text{II}}(\text{Me}_6\text{tren})\text{Cl}](\text{ClO}_4)$	Trigonal bipyramidal	-6.2	nr	nr	5
$[\text{Co}^{\text{II}}(\text{Me}_6\text{tren})\text{Br}](\text{ClO}_4)$	Trigonal bipyramidal	-2.5	nr	nr	5
$[\text{Co}(\text{NS}_3^{\text{tPr}})\text{Cl}](\text{BPh}_4)$	Trigonal bipyramidal	-23.0	32.0	$2.1 \times 10^{-11}$	6
$[\text{Co}(\text{NS}_3^{\text{tBu}})\text{Cl}]\text{ClO}_4$	Trigonal bipyramidal	-21.4	21.0	$4.6 \times 10^{-8}$	7
$[\text{Co}(\text{NS}_3^{\text{tBu}})\text{Br}]\text{ClO}_4$	Trigonal bipyramidal	-20.2	21.0	$4.6 \times 10^{-8}$	7
$[\text{Co}(\text{NS}_3^{\text{tBu}})\text{NCS}]\text{ClO}_4$	Trigonal bipyramidal	-11.0	20.0	$2.0 \times 10^{-9}$	7
$[\text{Co}^{\text{II}}(\text{Me}_4\text{cyclam})\text{N}_3]\text{ClO}_4$	Trigonal bipyramidal	46.7	nr	nr	8
$[\text{Co}(\text{TPMA})(\text{CH}_3\text{CN})](\text{BF}_4)_2 \cdot \text{CH}_3\text{CN}$	Trigonal bipyramidal	9.66	15.0	$1.7 \times 10^{-8}$	9
$[\text{Co}(\text{TPMA})\text{Cl}]\text{Cl}$	Trigonal bipyramidal	-8.49	16.4	$5.2 \times 10^{-8}$	9
$[\text{Co}(\text{TPMA})\text{Br}]\text{Br}$	Trigonal bipyramidal	-7.18	12.3	$8.0 \times 10^{-8}$	9
$[\text{Co}(\text{tpa})\text{Cl}]\cdot\text{ClO}_4$	Trigonal bipyramidal	-10.1	12.0	$7.2 \times 10^{-6}$	10
$[\text{Co}(\text{tpa})\text{Br}]\cdot\text{ClO}_4$	Trigonal bipyramidal	-7.8	8.7	$5.8 \times 10^{-6}$	10
$[\text{Co}(\text{tbta})\text{Cl}]\cdot(\text{ClO}_4)\cdot(\text{MeCN})_2\cdot(\text{H}_2\text{O})$	Trigonal bipyramidal	-7.5	8.1	$3.5 \times 10^{-6}$	10
$[\text{Co}(\text{tbta})\text{Br}]\cdot\text{ClO}_4$	Trigonal bipyramidal	-4.3	5.0	$2.1 \times 10^{-6}$	10
$[\text{Co}^{\text{II}}(\text{hdppy})\text{Cl}_2]$	Square pyramidal	151	9.4	$1.3 \times 10^{-7}$	11
$[\text{Co}^{\text{II}}(\text{DAPDPI})(\text{NCS})_2]$	Square pyramidal	-40.5	11.1	$3.6 \times 10^{-6}$	12
$[\text{Co}^{\text{II}}(\text{DBPDPI})(\text{NCS})_2]$	Square pyramidal	-40.6	16.6	$5.1 \times 10^{-7}$	12
$[\text{Co}(\text{bbp})\text{Cl}_2]\cdot(\text{MeOH})$	Square pyramidal	14.9	19.6	$5.8 \times 10^{-5}$	13
$[\text{Co}(\text{bbp})\text{Br}_2]\cdot(\text{MeOH})$	Square pyramidal	8.4	6.4	$3.1 \times 10^{-5}$	13

[Co(PP <sub>3</sub> )Cl]·ClO <sub>4</sub>	Square pyramidal	46.4	26.1	$8.2 \times 10^{-6}$	14
[Co(PP <sub>3</sub> )Br]·ClO <sub>4</sub>	Square pyramidal	40.7	23.9	$6.7 \times 10^{-6}$	14
[Co(14-TMC)Cl](BF <sub>4</sub> ) (1)	Square pyramidal	44.2	5.0	$2.7 \times 10^{-6}$	This paper
[Co(12-TBC)Cl](ClO <sub>4</sub> )·(MeCN) (2)	Square pyramidal	53.6	12.7	$3.2 \times 10^{-6}$	This paper

nr = not reported.

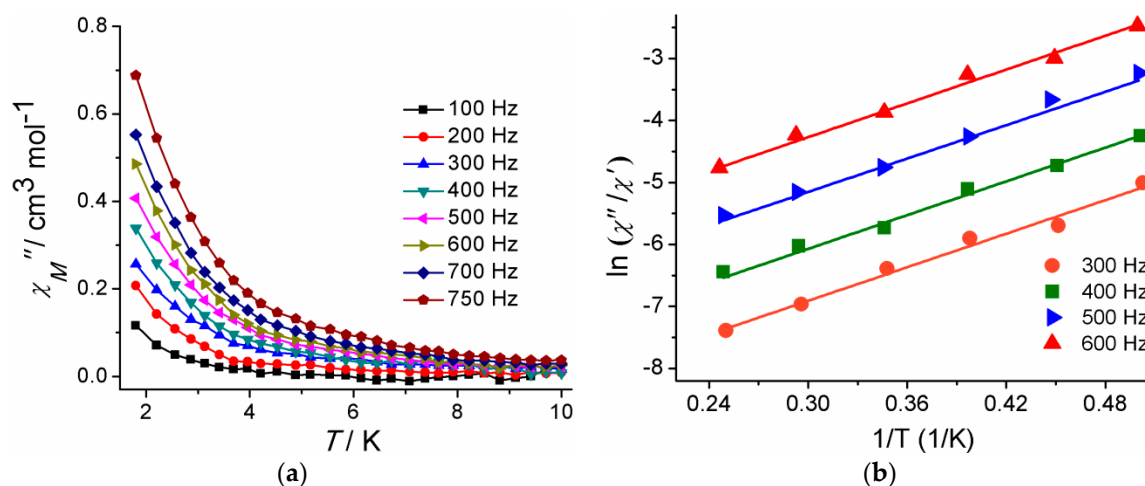


**Figure S7.** Temperature dependence of the out-of-phase ( $\chi_M''$ ) (a) AC magnetic susceptibility plots for complex 1 under 2000 Oe dc field; Natural logarithm of the ratio of  $\chi_M''$  over  $\chi_M'$  vs.  $1/T$  (b) for complex 1 (solid lines represent the best fit obtained from Equation (2) described in the main text).

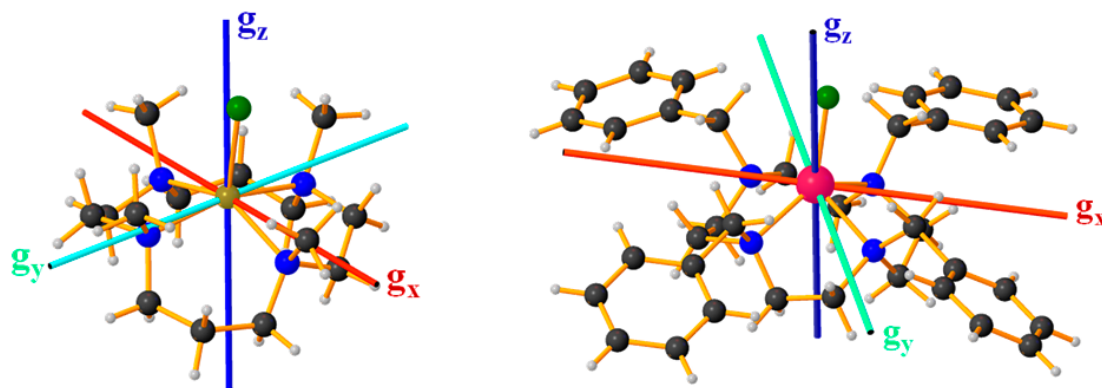


**Figure S8.** Orientation of the computed  $g$  tensor for complexes 1 (left) and 2 (right) with ORCA.

**Table S7.** Energy of the first four excited states ( $\text{cm}^{-1}$ ) and their contribution to the  $D$  and  $E$  values in  $\text{cm}^{-1}$  at CAS(7,5) NEVPT2 level by ORCA.

State	Mult	Complex 1			Complex 2		
		Energy	$D$	$E$	Energy	$D$	$E$
1st	4	1129	8.620	-6.926	768.3	47.398	40.233
2nd	4	2089	-2.392	0.221	1090.2	41.051	-30.688
3rd	4	2862	30.084	29.458	4116.3	1.825	1.712
4th	4	7278.2	8.422	-8.379	8311.1	-4.774	0.015
5th	4	9160.6	0.087	-0.087	8520.8	-0.631	-0.018
6th	4	10944.9	-0.077	0.008	10889.7	-6.708	0.017

## References

- Schweinfurth, D.; Sommer, M.G.; Atanasov, M.; Demeshko, S.; Hohloch, S.; Meyer, F.; Neese, F.; Sarkar, B. The Ligand Field of the Azido Ligand: Insights into Bonding Parameters and Magnetic Anisotropy in a Co(II)-Azido Complex. *J. Am. Chem. Soc.* **2015**, *137*, 1993, doi:10.1021/ja512232f.
- Boča, R.; Dlhán, L.U.; Linert, W.; Ehrenberg, H.; Fuess, H.; Haase, W. Ligand sphere-enhanced magnetic anisotropy in cobalt(II) and manganese(II) 2,6-bis-(benzimidazol-2'-yl)-pyridine dichloride. *Chem. Phys. Lett.* **1999**, *307*, 359 doi:10.1016/S0009-2614(99)00519-9.
- Rajnák, C.; Titiš, J.; Šalitraš, I.; Boča, R.; Fuhr, O.; Ruben, M. Zero-field splitting in pentacoordinate Co(II) complexes. *Polyhedron* **2013**, *65*, 122, doi:10.1016/j.poly.2013.08.029.
- Nemec, I.; Marx, R.; Herchel, R.; Neugebauer, P.; van Slageren, J.; Trávníček, Z. Field-induced slow relaxation of magnetization in a pentacoordinate Co(II) compound [Co(phen)(DMSO)Cl<sub>2</sub>]. *Dalton Trans.* **2015**, *44*, 15014, doi: 10.1039/C5DT02162F.
- Ruamps, R.; Batchelor, L.J.; Guillot, R.; Zakhia, G.; Barra, A.-L.; Wernsdorfer, W.; Guihéry, N.; Mallah, T. Ising-type magnetic anisotropy and single molecule magnet behaviour in mononuclear trigonal bipyramidal Co(II) complexes. *Chem. Sci.* **2014**, *5*, 3418, doi:10.1039/C4SC00984C].
- Shao, F.; Cahier, B.; Guihéry, N.; Rivière, E.; Guillot, R.; Barra, A.-L.; Lan, Y.; Wernsdorfer, W.; Campbell, V. E.; Mallah, T., Tuning the Ising-type anisotropy in trigonal bipyramidal Co(II) complexes. *Chem. Commun.* **2015**, *51*, 16475, doi:10.1039/C5CC07741A.
- Shao, F.; Cahier, B.; Rivière, E.; Guillot, R.; Guihéry, N.; Campbell, V.E.; Mallah, T., Structural Dependence of the Ising-type Magnetic Anisotropy and of the Relaxation Time in Mononuclear Trigonal Bipyramidal Co(II) Single Molecule Magnets. *Inorg. Chem.* **2017**, *56*, 1104, doi:10.1021/acs.inorgchem.6b01966.
- Cahier, B.; Perfetti, M.; Zakhia, G.; Naoufal, D.; El-Khatib, F.; Guillot, R.; Rivière, E.; Sessoli, R.; Barra, A.-L.; Guihéry, N.; Mallah, T. Magnetic Anisotropy in Pentacoordinate Ni<sup>II</sup> and Co<sup>II</sup> Complexes: Unraveling Electronic and Geometrical Contributions. *Chem. Eur. J.* **2017**, *23*, 3648, doi:10.1002/chem.201604872.
- Woods, T.J.; Ballesteros-Rivas, M.F.; Gómez-Coca, S.; Ruiz, E.; Dunbar, K.R. Relaxation Dynamics of Identical Trigonal Bipyramidal Cobalt Molecules with Different Local Symmetries and Packing Arrangements: Magnetostructural Correlations and ab initio Calculations. *J. Am. Chem. Soc.* **2016**, *138*, 16407, doi:10.1021/jacs.6b10154.
- Mondal, A.K.; Jover, J.; Ruiz, E.; Konar, S. Quantitative Estimation of Ising-Type Magnetic Anisotropy in a Family of C<sub>3</sub>-Symmetric Co<sup>II</sup> Complexes. *Chem. Eur. J.* **2017**, *23*, 12550, doi:10.1002/chem.201702108.
- Rajnák, C.; Titiš, J.; Fuhr, O.; Ruben, M.; Boča, R. Single-Molecule Magnetism in a Pentacoordinate Cobalt(II) Complex Supported by an Antenna Ligand. *Inorg. Chem.* **2014**, *53*, 8200, doi:10.1021/ic501524a.
- Jurca, T.; Farghal, A.; Lin, P.-H.; Korobkov, I.; Murugesu, M.; Richeson, D.S. Single-Molecule Magnet Behavior with a Single Metal Center Enhanced through Peripheral Ligand Modifications. *J. Am. Chem. Soc.* **2011**, *133*, 15814, doi:10.1021/ja204562m.
- Mondal, A.K.; Goswami, T.; Misra, A.; Konar, S. Probing the Effects of Ligand Field and Coordination Geometry on Magnetic Anisotropy of Pentacoordinate Cobalt(II) Single-Ion Magnets. *Inorg. Chem.* **2017**, *56*, 6870, doi:10.1021/acs.inorgchem.7b00233.
- Mondal, A.K.; Jover, J.; Ruiz, E.; Konar, S. Investigation of easy plane magnetic anisotropy in P-ligand square-pyramidal Co<sup>II</sup> single ion magnets. *Chem. Commun.* **2017**, *53*, 5338, doi:10.1039/C7CC02584J.